Mol Genet Genomics (2015) 290:1885–1897
DOI 10.1007/s00438-015-1047-1

ORIGINAL PAPER

MicroRNA expression profiles and networks in mouse lung infected with H1N1 influenza virus

Yanyan Bao[1] · Yingjie Gao[1] · Yahong Jin[1] · Weihong Cong[2] · Xin Pan[1] · Xiaolan Cui[1]

Received: 13 January 2015 / Accepted: 31 March 2015 / Published online: 18 April 2015

Abstract Influenza A viruses can cause localized outbreaks and worldwide pandemics, owing to their high transmissibility and wide host range. As such, they are among the major diseases that cause human death. However, the molecular changes induced by influenza A virus infection in lung tissue are not entirely clear. Changes in microRNA (miRNA) expression occur in many pathological and physiological processes, and influenza A virus infection has been shown to alter miRNA expression in cultured cells and animal models. In this study, we mined key miRNAs closely related to influenza A virus infection and explored cellular regulatory mechanisms against influenza A virus infection, by building networks among miRNAs and genes, gene ontologies (GOs), and pathways. In this study, miRNAs and mRNAs induced by H1N1 influenza virus infection were measured by gene chips, and we found that 82 miRNAs and 3371 mRNAs were differentially expressed. The 82 miRNAs were further analyzed with the series test of cluster (STC) analysis. Three of the 16 cluster profiles identified by STC, which include 46 miRNAs in the three profiles, changed significantly. Using potential target genes of the 46 miRNAs, we looked for intersections of these genes with 3371 differentially expressed mRNAs; 719 intersection genes were identified. Based on the GO or KEGG databases, we attained GOs or pathways for all of the above intersection genes. Fisher's and χ^2 test were used to calculate p value and false discovery rate (FDR), and according to the standard of $p < 0.001$, 241 GOs and 76 pathways were filtered. Based on these data, miRNA–gene, miRNA–GO, and miRNA–pathway networks were built. We then extracted three classes of GOs (related to inflammatory and immune response, cell cycle, proliferation and apoptosis, and signal transduction) to build three subgraphs, and pathways strictly related with H1N1 influenza virus infection were filtered to extract a subgraph of the miRNA-pathway network. Last, according to the pathway analysis and miRNA-pathway network analysis, 17 miRNAs were found to be associated with the "influenza A" pathway. This study provides the most complete miRNAome profiles, and the most detailed miRNA regulatory networks to date, and is the first to report the most important 17 miRNAs closely related with the pathway of influenza A. These results are a prelude to advancements in mouse H1N1 influenza virus infection biology and the use of mice as a model for human H1N1 influenza virus infection studies.

Keywords H1N1 · Influenza A virus · MicroRNA · Bioinformatics · STC analysis

Communicated by H. Siomi.

Electronic supplementary material The online version of this article (doi:10.1007/s00438-015-1047-1) contains supplementary material, which is available to authorized users.

✉ Xiaolan Cui
cuixiaolan2812@126.com; baoyanyan885@126.com

[1] Biosafety Laboratory, Institute of Chinese Materia Medica, China Academy of Chinese Medical Sciences, Beijing 100700, China

[2] Laboratory of Cardiovascular Diseases, Xiyuan Hospital, China Academy of Chinese Medical Sciences, Beijing 100091, China

Introduction

Influenza A viruses are negative-stranded RNA viruses that belong to the *Orthomyxoviridae* family. They can cause localized outbreaks and worldwide pandemics, owing to

their high transmissibility and wide host range. Even in non-pandemic years, influenza A viruses infect 5–15 % of the global population and result in >500,000 deaths yearly (Stöhr 2002). H1N1 influenza viruses are strong pathogenic subtype of influenza A viruses and H1N1 influenza viruses infecting humans are responsible for various illnesses, ranging from mild infection to severe pneumonia associated with acute respiratory distress syndrome. In 2009, human infection with a novel swine-origin H1N1 influenza virus spread rapidly to countries worldwide, leading the World Health Organization (WHO) to declare on 11 June 2009 the first influenza pandemic in more than 40 years (Butler 2010). Understanding the pathogenesis of H1N1 influenza virus infection is essential to preventing and controlling future outbreaks, but the molecular biological mechanisms of disease development are not entirely clear. Hence, it is crucial to explore molecular signaling pathways in H1N1 influenza virus infection. Influenza A virus infection has been shown to alter miRNA expression in cultured cells and animal models (Li et al. 2010, 2011; Loveday et al. 2012; Rogers et al. 2012; Wang et al. 2009, 2012; Skovgaard et al. 2013; Song et al. 2010; Terrier et al. 2013). Therefore, it is very important to explore the mechanism of miRNAs in H1N1 influenza virus infection and seek out miRNAs associated with influenza virus infection.

MicroRNAs (miRNAs) are noncoding single-stranded RNA molecules with a length of about 22nt, and are widespread in eukaryotic genomes. As a class of naturally occurring small and noncoding RNA molecules, miRNAs bind to the 3′ untranslated regions (3′-UTR) of target mRNAs, and either block translation or initiate transcript degradation (Cuellar and McManus 2005). miRNAs play a role in post-transcriptional regulation of gene expression through complementary binding to target mRNAs, and it is becoming increasingly evident that miRNAs are essential in many cellular processes, including cell proliferation, differentiation, apoptosis, and tumor formation. Host miRNAs can affect pathogenic processes through regulating host gene expression during influenza A virus infection (Li et al. 2010). In addition, because of the unique pathways of miRNAs, they have become a hot area of genetic research for the treatment of viral diseases.

In this study, we profiled miRNAs from the lung tissue of mice infected with H1N1 influenza virus at various time points. A total of 82 miRNAs were found to be differentially expressed in response to H1N1 influenza virus, including 46 miRNAs revealed by the series test of cluster (STC) analysis to play important roles and 17 miRNAs closely related to influenza A pathway. The 17 miRNAs have important value for further study of biological mechanisms, and some may be potential therapeutic targets for H1N1 influenza virus infection.

Materials and methods

Ethics statement

All procedures involving animals were approved by the Institutional Animal Care and Use Committee at the China Academy of Chinese Medical Sciences. The animal study was carried out in strict accordance with the recommendations in the Guide for the Care and Use of Laboratory Animals of the China Academy of Chinese Medical Sciences.

Virus

The virus strain used in this study was A/Puerto Rico/8/34 (PR8, H1N1) (ATCC, USA), a well-characterized, mouse-adapted laboratory strain of influenza A virus used as the genetic backbone for viruses from which inactivated influenza virus vaccines are generated. The virus was grown in the allantoic cavities of 10-day-old embryonated chicken eggs. Virus containing allantoic fluid was harvested and stored in aliquots at −80 °C until use. The 50 % tissue culture infections dose (TCID50) was determined by serial dilution of the virus in Madin–Darby canine kidney (MDCK) cells (ATCC) and calculated by the method developed by Reed and Muench (Neumann and Kawaoka 2001). All experiments with live influenza viruses were performed in a biosafety level-2 (BSL-2) laboratory.

Viral infections in mice

Specific pathogen-free 13–15 g male and female ICR mice were provided by the Beijing Vital River Laboratory Animal Technology Co., Ltd. PR8 virus infections in mice were conducted as described previously (Sun et al. 2011). Briefly, the mice were anesthetized with ether and were intranasally inoculated with 10^4 TCID50 of PR8 virus in physiological saline. Based on a pilot study, for the present study the weight loss, lung damage and histopathological changes were observed in mice infected with 10^4 TCID50 of PR8 virus. In addition, a normal control group was given intranasal physiological saline.

RNA isolation

For total RNA extraction, entire lungs from mice infected with PR8 virus ($n = 12$ per group) were randomly selected and harvested on the 2nd and 5th day. Entire lungs from 12 control mice were also randomly selected and harvested on the 5th day. Whole mouse lung tissues were homogenized in liquid nitrogen. Total RNA was extracted from mouse lungs using Qiagen miRNeasy Mini Kit (Qiagen, Germany).

MiRNA and mRNA microarray analysis

Total RNA was processed with miRNA and mRNA microarray analysis, using Affymetrix miRNA 4.0 and Affymetrix GeneChip Mouse 1.0 (Affymetrix, USA). There were three pools per group; each pool consisted of four mice. The random-variance model (RVM) *F* test was applied to filter differentially expressed genes for the control and infected groups, because the RVM *F* test is an efficient analysis method in cases of small samples. After the significance analysis and false discovery rate (FDR) analysis, differentially expressed genes were selected according to their *p* value threshold (Wright and Simon 2003; Yang et al. 2005; Clarke et al. 2008).

Bioinformatics analysis

A comprehensive bioinformatics analysis approach was used to enrich the dataset for genes, including the series test of cluster (STC) analysis, gene ontology (GO) analysis, pathway analysis, and gene, GO and pathway network analysis.

STC analysis

The STC algorithm of gene expression dynamics was used to profile the gene expression time series and to identify the most probable set of clusters. This method explicitly took into account the dynamic nature of temporal gene expression profiles during clustering, and identified a number of distinct clusters.

We selected differentially expressed genes according to RVM corrective analysis of variance (ANOVA). In accordance with different signal density changes tendency of genes under different situations, we identified a set of unique expression tendencies. The raw expression values were converted into a log2 ratio. Using a strategy for clustering time series gene expression data, we defined unique profiles. The expression profiles are related to the actual or expected number of genes assigned to each profile. Profiles that are significant have higher probability than expected by Fisher's exact test and multiple comparison tests (Xiao et al. 2010; Miller et al. 2002; Ramoni et al. 2002).

GO analysis

GO analysis was applied to analyze the main functions of genes with differential expression, according to Gene Ontology (the key functional classification of NCBI). GO analysis can organize genes into hierarchical categories and uncover the gene regulatory network based on biological processes and molecular functions (Gene Ontology Consortium 2006; Ashburner et al. 2000).

Two-sided Fisher's exact test and χ^2 test were used to classify GO categories, and FDR was calculated to correct the *p* value (Dupuy et al. 2007) (the smaller the FDR, the smaller the error in judging the *p* value). The FDR was defined as FDR $= 1 - N_k/T$, where N_k refers to the number of Fisher's test *p* values that are less than χ^2 test *p* values. We calculated *p* values for the GOs of every differential gene. Enrichment provides a measure of the significance of the function: as the enrichment increases, the corresponding function is more specific, which helps us to find GOs with more concrete functions in the experiment. Within the significant category, the enrichment *Re* was given by: $Re = (n_f/n)/(N_f/N)$, where "n_f" is the number of flagged genes within the particular category, "*n*" is the total number of genes within the same category, "N_f" is the number of flagged genes in the entire microarray, and "*N*" is the total number of genes in the microarray (Schlitt et al. 2003).

Pathway analysis

Pathway analysis was used to determine the significant pathway of the differential genes, according to KEGG, Biocarta, and Reactome. We used Fisher's exact test and the χ^2 test to select the significant pathway, and the threshold of significance was defined by *p* value and FDR. The enrichment Re was calculated as above (Kanehisa et al. 2004; Yi et al. 2006; Draghici et al. 2007).

MicroRNA–gene network

To build a miRNA–gene network, the relationships between miRNAs and genes were counted by their differential expression values, and according to their interactions in the Sanger miRNA database.

An adjacency matrix of miRNAs and genes $A = [ai, j]$ was made by the attribute relationships among genes and miRNA, where ai, j represents the weight of the relationship between gene *i* and miRNA *j*. In the miRNA–gene network, genes were represented by circles, miRNAs were represented by squares, and interactions were represented by edges. Using the methods of graph theory, we evaluated the regulatory status of miRNAs and genes; the evaluation criteria were the degrees of miRNAs and genes in the network. The degree of each miRNA was the number of genes regulated by that miRNA, and the degree of each gene was the number of miRNAs which regulated the gene. In this type of analysis, key miRNAs and genes in the network are those with the biggest degrees (Joung et al. 2007; Shalgi et al. 2007; Enright et al. 2003).

MicroRNA–GO network

A miRNA–GO network was built according to the relationships of significant GOs and genes, as well as the relationships among miRNAs and GOs. An adjacency matrix of miRNAs and genes $A = [ai, j]$ was made by the relationships among GOs and miRNAs, where ai, j represents the weight of the relationship between GO i and miRNA j. In the miRNA–GO network, a circle represents a GO, a square represents a miRNA, and relationships between them are represented by edges. Using the methods of graph theory, we evaluated the regulatory status of miRNAs and GOs; the evaluation criteria were the degrees of miRNAs and GOs in the network. The degree of each miRNA was the number of GOs regulated by that miRNA, and the degree of each GO was the number of miRNAs which regulated the GO. Key miRNAs and GOs in the network had the biggest degrees.

MicroRNA–pathway network

A miRNA–pathway network was built according to the relationship of significant pathways, genes, and the relationships among miRNAs and pathways. An adjacency matrix of miRNAs and genes $A = [ai, j]$ was made by the relationships among pathways and miRNAs, where ai, j represents the weight of the relationship between pathway i and miRNA j. In the miRNA–pathway network, a circle represents a pathway, a square represents a miRNA, and relationships between them are represented by edges. Using the methods of graph theory, we evaluated the regulatory status of miRNAs and pathways; the evaluation criteria were the degrees of miRNAs and pathways in the network. The degree of each miRNA was the number of pathways regulated by that miRNA, and degree of each pathway was the number of miRNAs that regulated the pathway. Key miRNAs and pathways in the network had the biggest degrees.

Table 1 Lung index of mice after PR8 virus infection

Groups	Survival rate (%)	Weight loss rate (%)	Lung index (%)	
			Average	Standard deviation
Control	100	–	0.77	0.05
2-day	100	25	0.97**	0.07
5-day	100	38	1.93**, ##	0.47

** vs. control group, $p < 0.01$; ## vs. 2-day group, $p < 0.01$

Histopathologic analysis

Lungs were fixed in 4 % formalin, dehydrated in ascending ethanol concentrations, embedded in paraffin, sectioned into 4 μm slices, and stained with hematoxylin and eosin (H&E). Histopathology photos were taken using a phase inverted microscope (Olympus, Japan).

Real-time RT-PCR

Real-time reverse-transcription polymerase chain reaction (RT-PCR) was performed to measure the levels of miR-3473f in profile 1, miR-21a-3p in profile 11, and miR-92b-3p in profile 15. A total of 0.5 μg of total RNA was reverse transcribed using M-MLV reverse transcriptase (Thermo, USA) with a special stem-loop primer (Genepharma, China) for miR-3473f, miR-21a-3p and miR-92b-3p. Real-time RT-PCR was performed on a Thermo PikoReal Real-Time PCR system (Thermo, USA) using the Hairpin-it miRNA detection kit (Genepharma, China). All samples were analyzed in triplicate, including a no-template control. The relative expression level was determined by the $2^{-\Delta\Delta Ct}$ method and normalized to U6 expression.

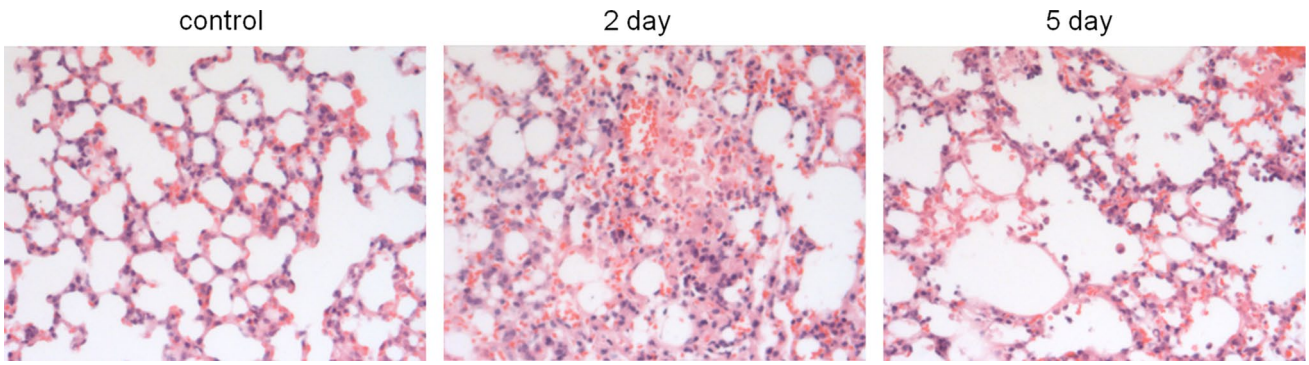

Fig. 1 Hematoxylin and eosin staining to evaluate histopathological inflammatory changes. Compared with the control group, significant inflammatory infiltration appeared in the 2-day and 5-day groups

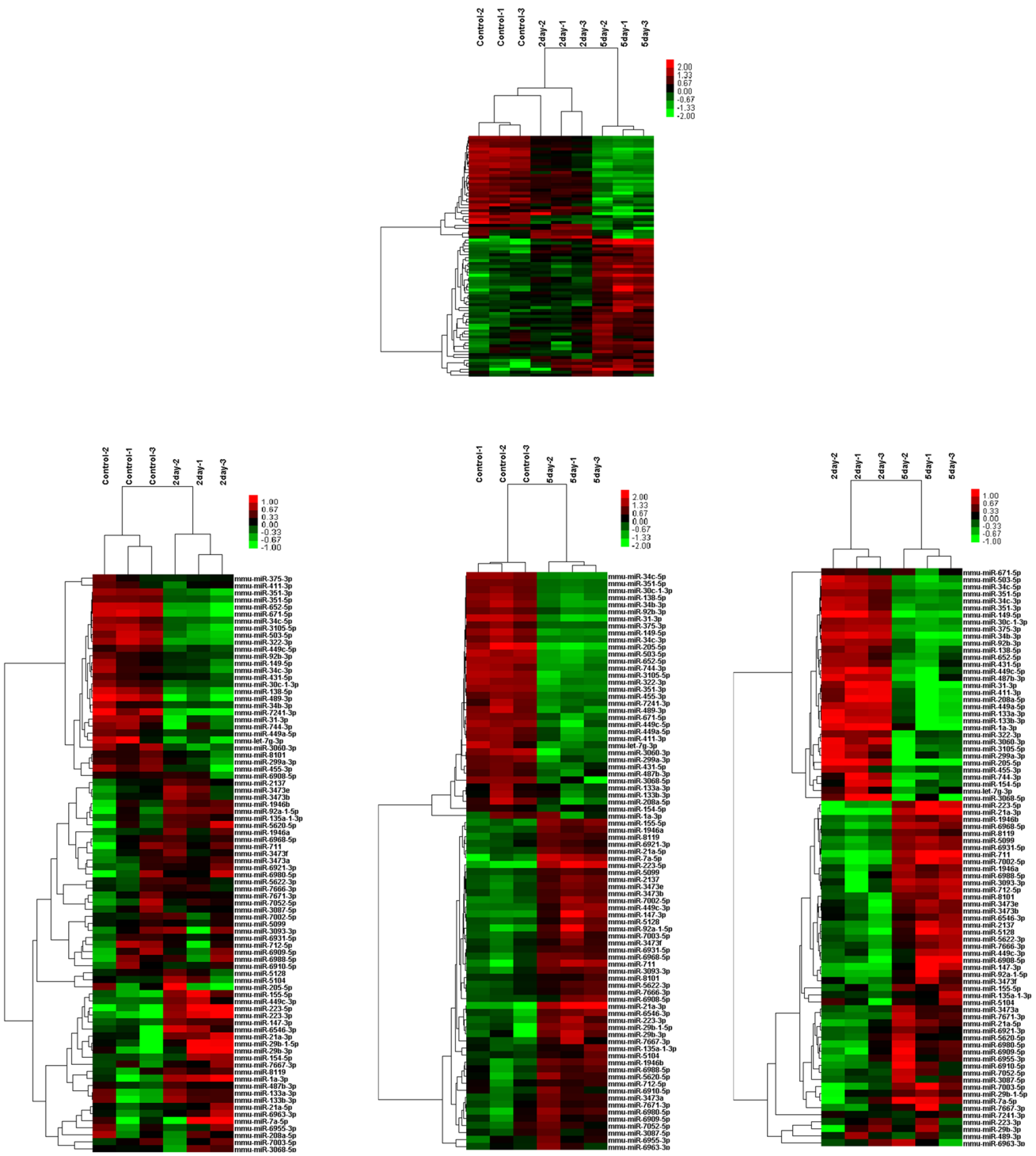

Fig. 2 MiRNA profiles differentiate the lung of mice with PR8 viral infection (2-day and 5-day) from the lung of mice with no viral infection (control). Both down-regulated (*green*) and up-regulated (*red*) miRNAs were identified in infected lungs (color figure online)

Statistical analysis

The lung index results were expressed as mean ± standard deviation (SD). Statistical analysis was done with ANOVA for multiple comparisons. Differences with $p < 0.05$ were considered statistically significant.

Table 2 Sixteen of STC profiles

Profile number	Control	2-day	5-day	Genes_ assigned	Adj_*p* value
1	**0**	**1**	**2**	**17**	**1.82E−06**
2	0	2	3	10	0.078567
3	0	1	1	3	1
4	0	−1	−2	4	1
5	0	2	1	0	1
6	0	−1	0	0	1
7	0	−2	−3	0	1
8	0	−2	−1	0	1
9	0	−1	−3	8	0.606619
10	0	−1	1	0	1
11	**0**	**1**	**3**	**15**	**2.12E−06**
12	0	1	0	4	1
13	0	−1	−1	3	1
14	0	0	1	2	1
15	**0**	**0**	**−1**	**14**	**0.029759**
16	0	1	−1	2	1

Significant STC is marked in bold

Table 3 MiRNAs included in profile 1

miRNA	Control	2-day	5-day	Profile number
mmu-miR-1946a	0	1.028305	2.00168	1
mmu-miR-1946b	0	1.187406	2.151776	1
mmu-miR-2137	0	0.911687	2.063735	1
mmu-miR-21a-5p	0	0.886565	1.870083	1
mmu-miR-3473a	0	0.951963	1.661932	1
mmu-miR-5622-3p	0	0.695266	1.602789	1
mmu-miR-3473e	0	1.09161	2.068612	1
mmu-miR-3473b	0	0.964588	1.849079	1
mmu-miR-7666-3p	0	0.673894	1.46227	1
mmu-miR-147-3p	0	1.211252	2.833279	1
mmu-miR-92a-1-5p	0	1.462468	2.880418	1
mmu-miR-3473f	0	0.855149	1.60495	1
mmu-miR-6980-5p	0	1.050828	2.04166	1
mmu-miR-7667-3p	0	0.981042	1.816474	1
mmu-miR-7a-5p	0	1.39438	3.144593	1
mmu-miR-6955-3p	0	0.58184	1.337931	1
mmu-miR-7052-5p	0	0.698893	1.320691	1

Results

Mouse model of PR8 virus infection

Survival rate, weight loss rate, lung index, and histopathology were used to evaluate the degree of mouse lung damage by the PR8 virus. Survival rate was calculated by the following formula: survival rate (%) = (number of surviving mice/number of test mice) × 100 %. Weight loss was calculated by the following formula: weight loss rate (%) = [weight (control) − weight (infection)]/weight (control) × 100 %. The lung index of mice was calculated by

Table 4 MiRNAs included in profile 11

miRNA	Control	2-day	5-day	Profile number
mmu-miR-5099	0	0.4963	1.662804	11
mmu-miR-21a-3p	0	1.688131	4.185962	11
mmu-miR-6931-5p	0	0.491164	1.556557	11
mmu-miR-6968-5p	0	0.799548	2.049541	11
mmu-miR-7002-5p	0	0.539259	2.322859	11
mmu-miR-5128	0	0.567899	1.902259	11
mmu-miR-711	0	1.066991	2.997127	11
mmu-miR-7671-3p	0	0.618608	1.494586	11
mmu-miR-7003-5p	0	0.436771	1.9175	11
mmu-miR-6908-5p	0	0.324857	1.685382	11
mmu-miR-3093-3p	0	0.553106	2.009915	11
mmu-miR-6988-5p	0	0.667645	1.703633	11
mmu-miR-6910-5p	0	0.468667	1.359976	11
mmu-miR-6909-5p	0	0.480588	1.469696	11
mmu-miR-3087-5p	0	0.395531	0.975955	11

Table 5 MiRNAs included in profile 15

miRNA	Control	2-day	5-day	Profile number
mmu-miR-30c-1-3p	0	−0.12143	−1.26038	15
mmu-miR-34b-3p	0	−0.08411	−1.74717	15
mmu-miR-92b-3p	0	0.129891	−1.08129	15
mmu-miR-149-5p	0	−0.03333	−1.79601	15
mmu-miR-375-3p	0	0.317032	−0.97915	15
mmu-miR-34c-3p	0	−0.1853	−1.31436	15
mmu-miR-449a-5p	0	0.074039	−1.37899	15
mmu-miR-449c-5p	0	−0.03664	−1.71842	15
mmu-miR-411-3p	0	0.218616	−1.22654	15
mmu-miR-431-5p	0	0.184807	−0.82167	15
mmu-miR-744-3p	0	−0.26914	−1.60234	15
mmu-miR-205-5p	0	0.665344	−2.83009	15
mmu-miR-208a-5p	0	0.431046	−1.30526	15
mmu-miR-299a-3p	0	−0.04044	−1.15337	15

the following formula: lung index (%) = (lung weight/body weight) × 100 %. The survival rate of both the 2-day and 5-day groups was 100 %, and the weight loss rate of the 2-day and 5-day groups were 25 and 38 %, respectively. The lung index of the control, 2-day, and 5-day groups were 0.77 ± 0.05, 0.97 ± 0.07, and 1.93 ± 0.47, respectively. Compared with the control group, the lung index of both infection groups was significantly higher ($p < 0.01$); compared with the 2-day group, the lung index of the 5-day group was also significantly higher ($p < 0.01$) (Table 1). H&E staining was performed to compare histopathological inflammatory changes. Compared with the control group, significant inflammatory infiltration appeared in 2-day and 5-day groups (Fig. 1). The results showed that when mice were infected with 10^4TCID50 of PR8 virus, the mortality rate is zero at both 2 and 5 days after infection, and weight loss and lung damage increased with time.

Microarray data

A total of 82 miRNAs and 3371 mRNAs were significantly expressed ($p < 0.05$), and differences in miRNA (Fig. 2) and mRNA (data not shown) expression among groups were found.

Significant STC

The STC algorithm of miRNA expression dynamics was used to profile the 82 differentially expressed miRNAs ($p < 0.05$) and to identify the most probable set of

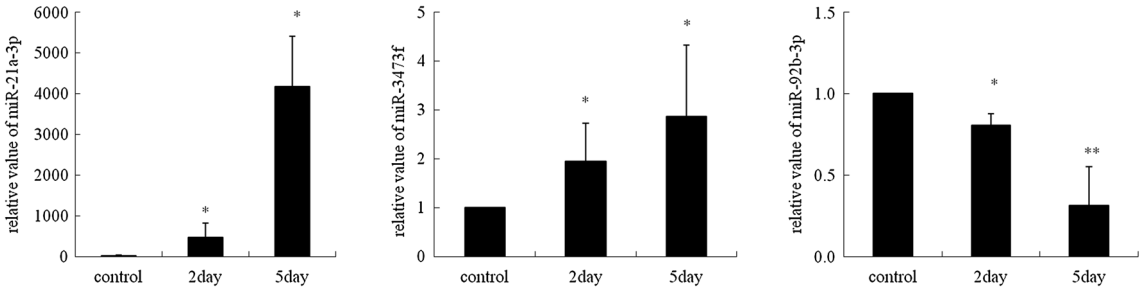

Fig. 3 Real-time RT-PCR was performed to verify the levels of miR-3473f (profile 1), miR-21a-3p (profile 11), and miR-92b-3p (profile 15). Expression changes are in the *same direction* as determined by the miRNA microarray ($n = 3$, $^*p < 0.05$, $^{**}p < 0.01$)

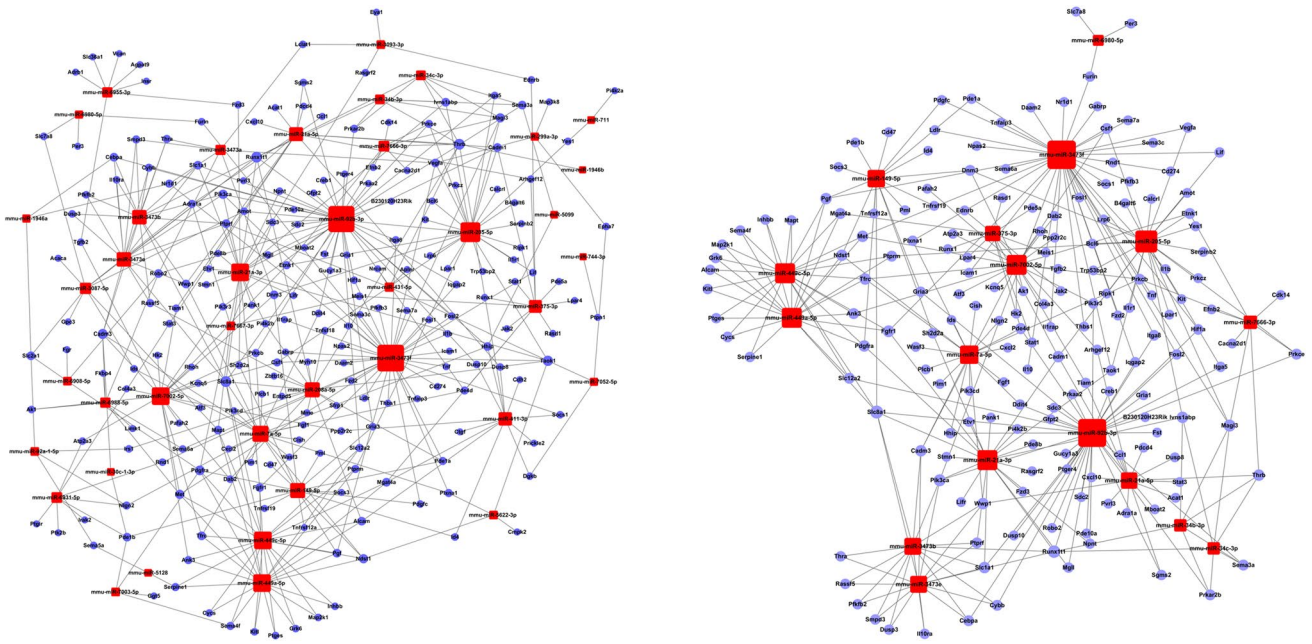

Fig. 4 A miRNA–gene network was built according to interactions between miRNAs and genes. *Red box nodes* denote miRNAs, *blue circle nodes* denote genes, and *edges* show the inhibitory effect of miRNAs on genes. *Left graph* full map of relationship between miRNAs and genes. *Right graph* miRNA–gene network subgraph. MiRNAs were derived from the influenza A pathway. The larger the area of the *box* or *circle*, the bigger is the degree of the miRNA or gene (color figure online)

clusters generated in the time series. STC analysis was used to place the 82 differentially expressed miRNAs into 16 expression pattern profiles (Figure S1; Table 2). The horizontal axis represents time points, 2-day located in 1.0 and 5-day located in 2.0; the vertical axis represents expression change (log2 ratio). Profile 1, profile 11 and profile 15 were confirmed to be significant STC clusters ($p < 0.05$). The p value of profile 1, which includes 17 miRNAs, was 1.82E − 06, and the expression change of the control, 2-day, and 5-day groups was 0, 1, and 2, respectively (Figures S1, S2; Tables 2, 3). The p value of profile 11, which includes 15 miRNAs, was 2.12E − 06, and the expression change of the control, 2-day, and 5-day groups was 0, 1, and 3, respectively (Figures S1, S3; Tables 2, 4). The p value of profile 15, which includes 14 miRNAs, was 0.029758, and the expression change of the control, 2-day, and 5-day groups was 0, 0, and −1, respectively (Figures S1, S4; Tables 2, 5). The STC method explicitly took into account the temporal nature of the miRNA expression profiles during clustering, and identified the number of distinct clusters. As a result, miRNAs in profile 1, profile 11 and profile 15 were confirmed to be more significant and valuable.

Verification of miRNAs microarray with real-time RT-PCR

We chose one miRNA per significant profile to validate by real-time RT-PCR: miR-3473f in profile 1, miR-21a-3p in profile 11, and miR-92b-3p in profile 15. The real-time

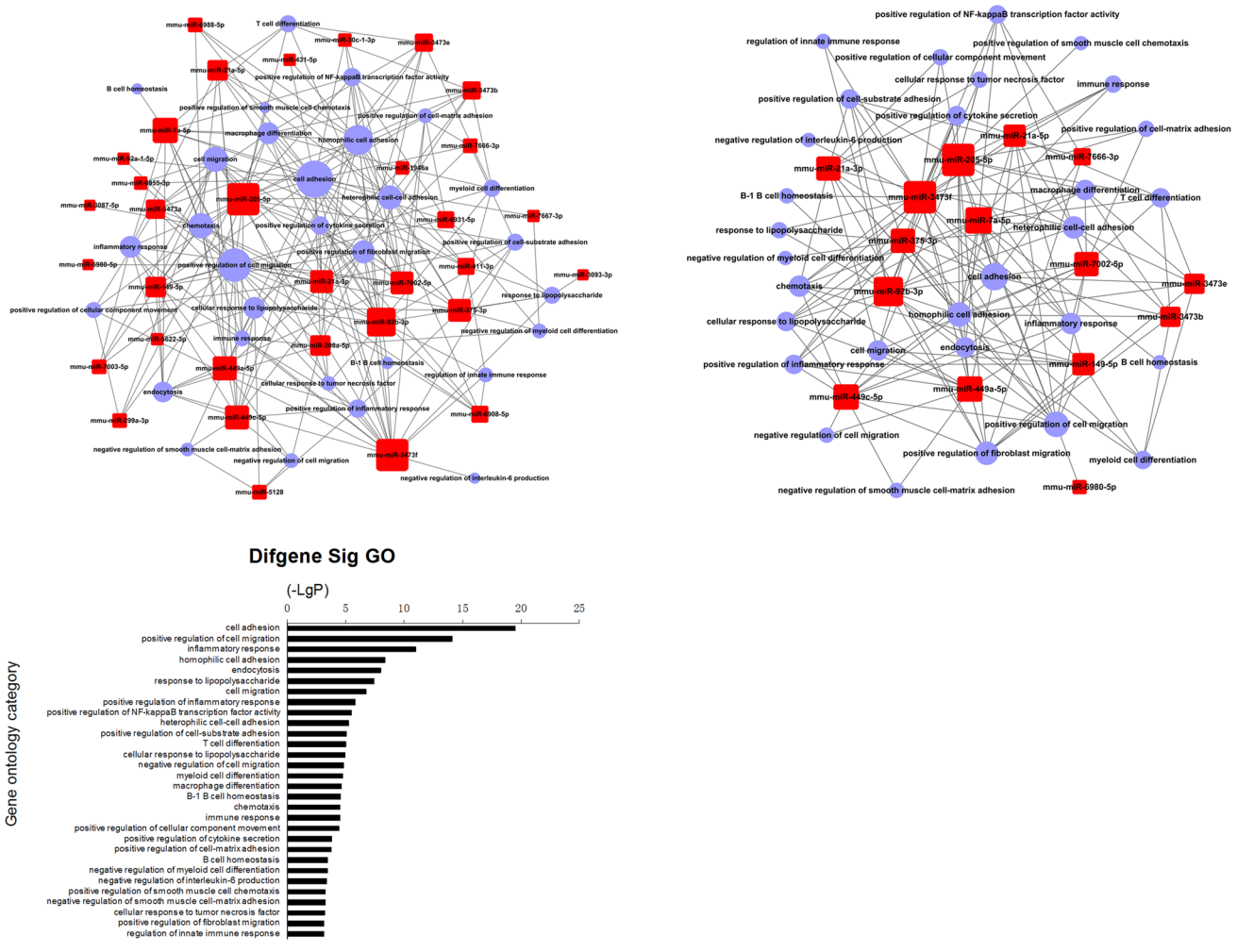

Fig. 5 A miRNA–GO network was built according to interactions between miRNAs and GOs. *Red box nodes* denote miRNAs, *blue circle nodes* denote GOs, and *edges* show the inhibitory effect of miRNAs on GOs. *Left network* miRNA–GO subgraph pertaining to inflammatory and immune response, with the histogram of significant GOs below. The *vertical axis* represents the GO category, and the *horizontal axis* represents –lg (p value) of the GO (the higher the value, the greater the GO significance level). *Right network* extracted from the network on the *left*, and including miRNAs which are derived from the influenza A pathway. The larger the area of *box* or *circle*, the bigger is the degree of the miRNA or GO

RT-PCR results showed that the expression changes of these three miRNAs are in the same direction as determined by the miRNA microarray ($p < 0.05$) (Fig. 3).

Gene ontology (GO) and pathway analysis

GO and pathway analyses were applied to analyze the main functions and significant pathways of the genes that were differentially expressed. Using bioinformatics algorithms, we searched for potential target genes of 46 differentially expressed miRNAs that were identified in the STC analysis. We then looked for intersections of these genes with 3371 differentially expressed mRNAs; 719 intersection genes were identified. The mRNAs that had a negative correlation with the above miRNAs were analyzed and listed (Table S1). According to the GO or KEGG databases, we gained GOs or pathways for all 719 intersection genes. Fisher's exact test and χ^2 test were used to calculate the p value and FDR of each GO and pathway. According to the standard of $p < 0.001$, 241 GOs and 76 pathways were filtered (Tables S2, S3), indicating that these GOs and pathways could be key in influenza A infection.

MiRNA regulatory networks of genes, GOs, or pathways

Building miRNAs regulatory networks could be very important for high-throughput analysis of interactions among miRNAs and genes, GOs, or pathways.

A miRNA–gene network was built according to interactions between miRNAs and genes in the Sanger miRNA database (Fig. 4). MiRNAs were derived from the significant STC profiles and genes were identified from the intersection between potential target genes of these miRNAs and 3371 differentially expressed mRNAs.

A miRNA–GO network was built according to relationships among significant GOs and genes and relationships among miRNAs and genes (Figure S5). MiRNAs were derived from the significant STC profiles and the 241 GOs were derived from the GO analysis. In addition,

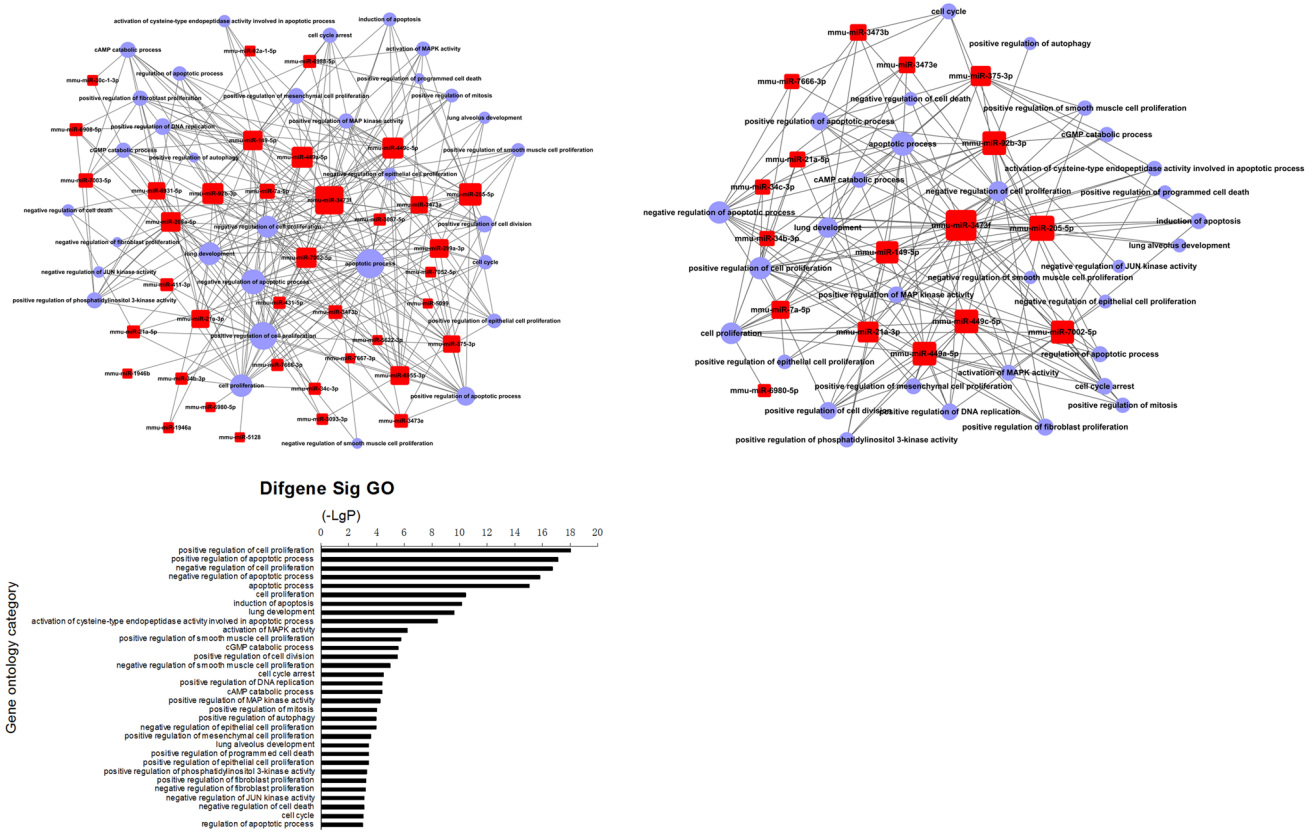

Fig. 6 A miRNA–GO network was built according to interactions between miRNAs and GOs. *Red box nodes* denote miRNAs, *blue circle nodes* denote GOs, and *edges* show the inhibitory effect of miRNAs on GOs. *Left network* miRNA–GO subgraph pertaining to cell cycle, proliferation and apoptosis, with the histogram of significant GOs below. The *vertical axis* represents the GO category; the *horizontal axis* represents –lg (p value) of the GO (the higher the value, the greater the GO significance level). *Right network* extracted from the network on the left, and including miRNAs which are derived from the influenza A pathway. The larger the area of *box* or *circle*, the bigger is the degree of the miRNA or GO

three classes of GOs related to inflammatory and immune response, cell cycle, proliferation and apoptosis, and signal transduction were extracted to build three subgraphs (Figs. 5, 6, 7).

A miRNA–pathway network was built according to relationships among significant pathways and genes and relationships among miRNAs and genes (Figure S6). MiRNAs were derived from the significant STC profiles, the 76 pathways were identified through the pathway analysis. In addition, pathways related to influenza A infection were filtered to develop a subgraph miRNA–pathway network (Fig. 8). Some pathways related to influenza A infection are associated with inflammatory and immune responses, such as cell adhesion molecules (CAMs), cytokine–cytokine receptor interactions, influenza A (http://www.genome.jp/dbget-bin/www_bget?pathway:map05164), chemokine signaling, NF-kappa B signaling, Toll-like receptor signaling, and TGF-beta signaling, and some pathways are associated with pathological processes of lesions in lung tissue, such as MAPK signaling, calcium signaling, PI3K-Akt signaling, and apoptosis.

These networks provided a large amount of information about the regulation of miRNAs in mouse lung infected with PR8 virus.

Analysis of miRNAs related to the influenza A pathway

In the miRNA–pathway network, there were 17 edges out of influenza A, so the influenza A pathway was regulated by 17 miRNAs (Table 6). Based on these 17 miRNAs, we extracted a miRNA–gene network subgraph (Fig. 4), miRNA–GO network subgraphs (Figs. 5, 6, 7), and a miRNA–pathway network subgraph (Fig. 8). These network subgraphs provide clues for in-depth study of the regulation of miRNAs, genes, and GOs related to the influenza A pathway.

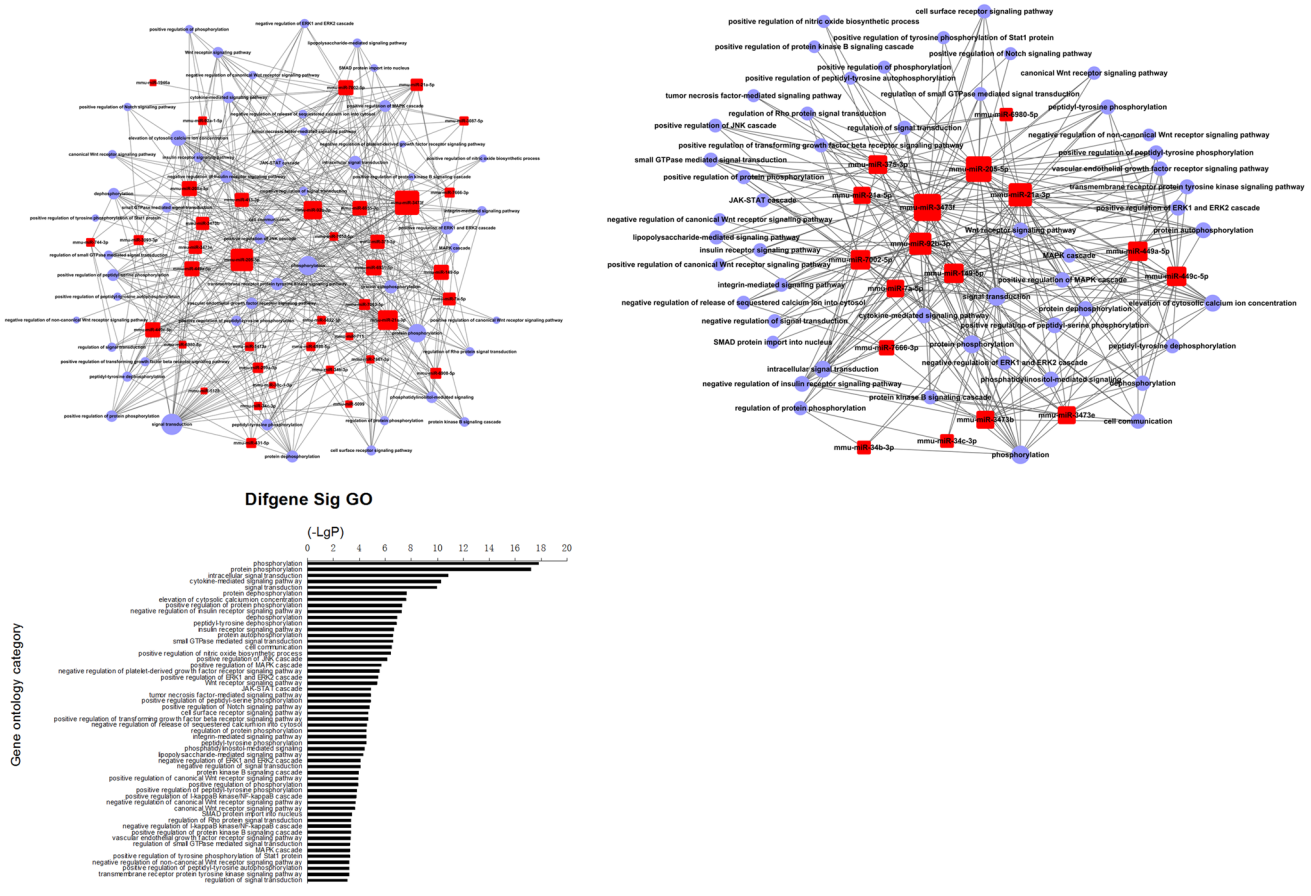

Fig. 7 A miRNA–GO network was built according to interactions between miRNAs and GOs. *Red box nodes* denote miRNAs, *blue circle nodes* denote GOs, and *edges* show the inhibitory effect of miRNAs on GOs. *Left network* miRNA–GO subgraph pertaining to signal transduction, with the histogram of significant GOs below. The *vertical axis* represents the GO category; the *horizontal axis* represents –lg (*p* value) of the GO (the higher the value, the greater the GO significance level). *Right network* extracted from the network on the left, and including miRNAs which are derived from the influenza A pathway. The larger the area of *box* or *circle*, the bigger is the degree of the miRNA or GO

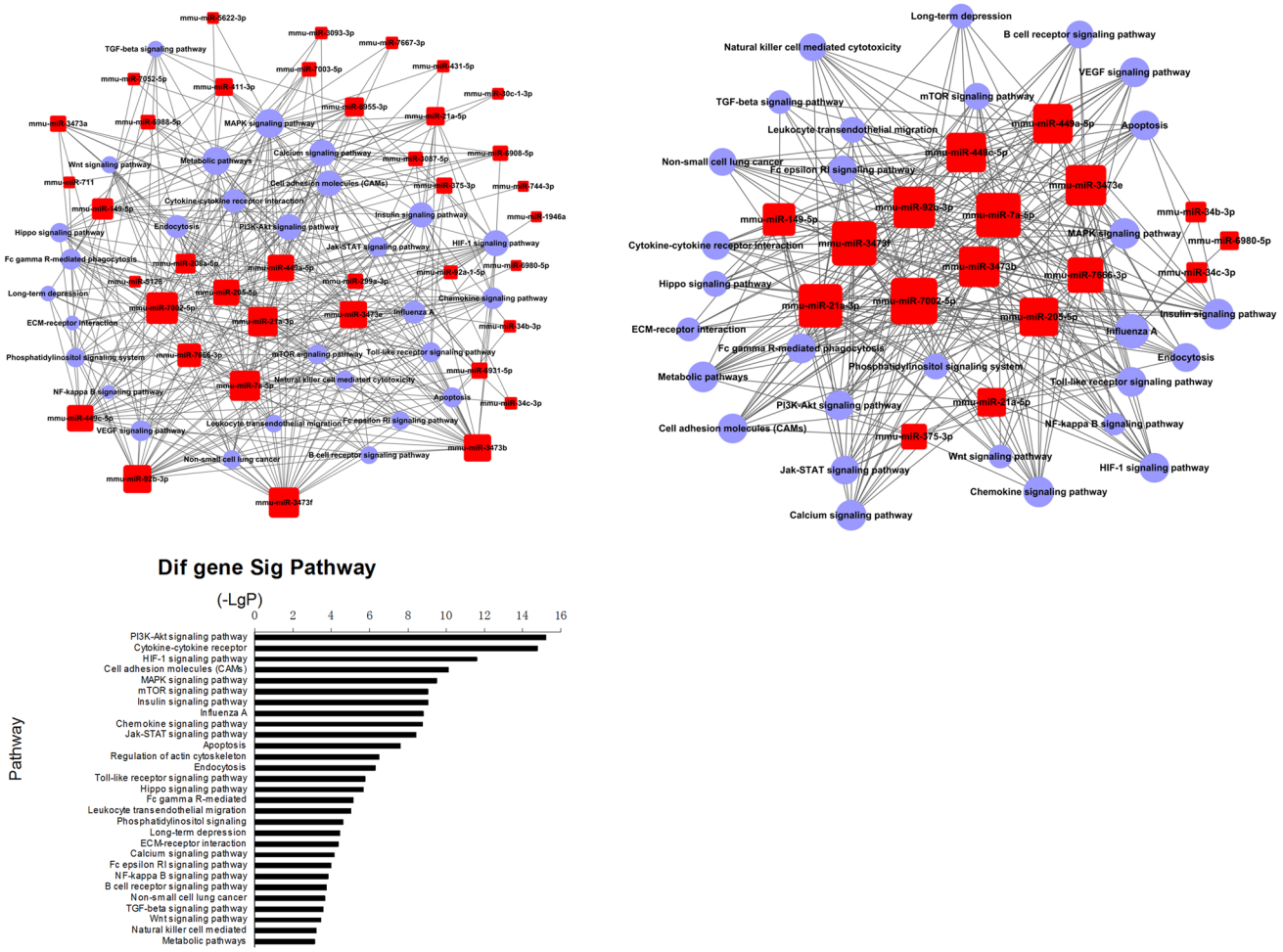

Fig. 8 A miRNA–pathway network was built according to interactions between miRNAs and pathways. *Red box nodes* denote miRNA, *blue circle nodes* denote pathways, and *edges* show the inhibitory effect of miRNA on pathways. *Left graph* pathways strictly related to influenza A infection were filtered to identify a miRNA–pathway network subgraph. The histogram of significant pathways is below. The *vertical axis* represents the pathway category; the *horizontal axis* represents –lg (*p* value) of the pathway (the higher the value, the greater the pathway significance level). *Right network* extracted from the left network, and including miRNAs which are derived from the influenza A pathway. The larger the area of *box* or *circle*, the bigger is the degree of the miRNA or pathway (color figure online)

Discussion

An influenza pandemic could bring great damage to human health and the global economy. Since the 19th century, there have been five global influenza pandemics, and during the "Spanish flu" H1N1 pandemic of 1918, nearly 50 million people died. The most recent influenza pandemic happened in 2009, and it was the first in more than 40 years (Butler 2010). Changes in miRNA expression occur in many pathological and physiological processes, and many previous studies have revealed that H1N1 virus infection can alter host miRNA expression. In this study, we investigated miRNA and mRNA expression induced by H1N1 influenza virus infection, and found that 82 miRNAs and 3371 mRNAs were expressed differently. We further analyzed the 82 miRNAs with STC analysis, and found that the expression of 46 miRNAs was significantly changed upon influenza infection. In addition, we found potential target genes of the 46 miRNAs using bioinformatics algorithms, and obtained 719 genes. Based on the GO and KEGG databases, we identified 241 GOs and 76 pathways. From these data we built miRNA–gene, miRNA–GO, and miRNA–pathway networks. Furthermore, 17 miRNAs were found to regulate the pathway of influenza A. This study provided the most comprehensive data to explore the mechanism of miRNAs in influenza A virus infection, and is the first to discover 17 miRNAs closely related to the pathway "Influenza A". These results lay a foundation and provide ideas for future in-depth studies, particularly related to the 17 miRNAs closely related with the influenza A pathway.

Table 6 MiRNAs related to the influenza A pathway

miRNA	Control	2-day	5-day	Profile number
mmu-miR-21a-5p	0	0.886565	1.870083	1
mmu-miR-3473e	0	1.09161	2.068612	1
mmu-miR-3473b	0	0.964588	1.849079	1
mmu-miR-7666-3p	0	0.673894	1.46227	1
mmu-miR-3473f	0	0.855149	1.60495	1
mmu-miR-6980-5p	0	1.050828	2.04166	1
mmu-miR-7a-5p	0	1.39438	3.144593	1
mmu-miR-21a-3p	0	1.688131	4.185962	11
mmu-miR-7002-5p	0	0.539259	2.322859	11
mmu-miR-34b-3p	0	−0.08411	−1.74717	15
mmu-miR-92b-3p	0	0.129891	−1.08129	15
mmu-miR-149-5p	0	−0.03333	−1.79601	15
mmu-miR-375-3p	0	0.317032	−0.97915	15
mmu-miR-34c-3p	0	−0.1853	−1.31436	15
mmu-miR-449a-5p	0	0.074039	−1.37899	15
mmu-miR-449c-5p	0	−0.03664	−1.71842	15
mmu-miR-205-5p	0	0.665344	−2.83009	15

Tan et al. profiled miRNA and mRNA expression levels following lung injury and tissue regeneration using a murine influenza pneumonia model. They found that miR-290 and miR-505 at 7 dpi and let-7, miR-21, and miR-30 at 15 dpi were highly involved in targeting gene functions related to tissue repair (Tan et al. 2014). Tambyah et al. used blood samples of influenza-infected patients and healthy controls, and found 14 highly dysregulated miRNAs that provided a clear distinction between infected and healthy individuals. Of these, expression of miR-1260, miR-26a, miR-335*, miR-576-3p, miR-628-3p and miR-664 were consistently dysregulated in both whole blood and H1N1-infected cells. These highly dysregulated miRNAs may have crucial roles in influenza pathogenesis, and are potential biomarkers of influenza (Tambyah et al. 2013). To further understand the molecular pathogenesis of the 2009 pandemic H1N1 influenza virus, Wu et al. profiled cellular miRNA of lungs from BALB/c mice infected with wild-type 2009 pandemic influenza virus A/Beijing/501/2009 (H1N1), and also included PR8 virus for comparison. Wu et al. reported 47 differentially expressed miRNAs from infections of both virus strains, including 29 for BJ501 and 43 for PR8. Among these, 15 miRNAs had no reported function, and 32 (including miR-155 and miR-233) are known to play important roles in cancer, immunity and antiviral activity (Wu et al. 2013). Li et al. (2010) found that a group of miRNAs, including miR-200a and miR-223, were differentially expressed in response to influenza virus infection and that r1918 and A/Texas/36/91 infection induced distinct miRNA expression profiles. However, previous studies have not systematically investigated the regulatory role of miRNA for pathways, but simply studied the enrichment of pathways. In H1N1 virus infection biology, the role of pathways is just as important as functions, and the regulation of miRNAs to GOs and pathways should be performed simultaneously. In this study, based on the three significant clusters of 46 differentially expressed miRNAs, we performed GO and pathway analysis to identify significant GOs and pathways, and built miRNA–gene, miRNA–GO, and miRNA–pathway networks to reveal miRNA regulation of genes, GOs, and pathways. Of note, 17 miRNAs that regulate the pathway of influenza A were identified. Although the expression of some of the 17 miRNAs or the family members of the 17 miRNAs were reported to significantly change in H1N1 virus infection, such as miR-21, miR-7a, miR-449a, and miR-34a (Wu et al. 2013; Li et al. 2010), the regulatory mechanism on pathways has not been studied previously; thus, we focused on the 17 miRNAs for further analysis. Based on these 17 miRNAs, we generated subgraphs of miRNA–gene, miRNA–GO, and miRNA–pathway networks. These subgraphs can clarify the biological effects of these 17 miRNAs in H1N1 virus infection and provide research ideas for further study.

This study provides not only the most complete miRNAome profiles for evaluating miRNAs abundance; it also provides the most detailed miRNA regulatory networks, targeting genes, GOs, and pathways for exploring the miRNA mechanisms in H1N1 influenza virus infection at specific time points in mice. Identification of these key miRNAs through bioinformatics analysis provides an initial group of expressed miRNAs that change in abundance during specific developmental stages and, therefore, may target on genes that regulate this process. It is worth noting that this is the first report of these 17 miRNAs being able to regulate the pathway “influenza A”, and all or some of these 17 miRNAs are of great research value. These results are a prelude to advancements in mouse H1N1 influenza virus infection biology, as well as the use of mice as model organism for human H1N1 influenza virus infection studies.

Acknowledgments This work is supported by the China Academy of Chinese Medical Sciences Foundation (No. ZZ2014010, No. ZZ2014040). The authors would like to thank Li Jing from Gminix Company for technical assistance.

References

Ashburner M, Ball CA, Blake JA, Botstein D, Butler H, Cherry JM, Davis AP, Dolinski K, Dwight SS, Eppig JT, Harris MA, Hill DP, Issel-Tarver L, Kasarskis A, Lewis S, Matese JC, Richardson JE, Ringwald M, Rubin GM, Sherlock G (2000) Gene ontology: tool for the unification of biology. The Gene Ontology Consortium. Nat Genet 25:25–29

Butler D (2010) Portrait of a year-old pandemic. Nature 464:1112–1113

Clarke R, Ressom HW, Wang A, Xuan J, Liu MC, Gehan EA, Wang Y (2008) The properties of high-dimensional data spaces: implications for exploring gene and protein expression data. Nat Rev Cancer 8:37–49

Cuellar TL, McManus MT (2005) MicroRNAs and endocrine biology. J Endocrinol 187:327–332

Draghici S, Khatri P, Tarca AL, Amin K, Done A, Voichita C, Georgescu C, Romero R (2007) A systems biology approach for pathway level analysis. Genome Res 17:1537–1545

Dupuy D, Bertin N, Hidalgo CA, Venkatesan K, Tu D, Lee D, Rosenberg J, Svrzikapa N, Blanc A, Carnec A, Carvunis AR, Pulak R, Shingles J, Reece-Hoyes J, Hunt-Newbury R, Viveiros R, Mohler WA, Tasan M, Roth FP, Le Peuch C, Hope IA, Johnsen R, Moerman DG, Barabási AL, Baillie D, Vidal M (2007) Genome-scale analysis of in vivo spatiotemporal promoter activity in *Caenorhabditis elegans*. Nat Biotechnol 25:663–668

Enright AJ, John B, Gaul U, Tuschl T, Sander C, Marks DSM (2003) MicroRNA targets in *Drosophila*. Genome Biol 5:R1

Gene Ontology Consortium (2006) The gene ontology (GO) project in 2006. Nucleic Acids Res 34:D322–D326

Joung JG, Hwang KB, Nam JW, Kim SJ, Zhang BT (2007) Discovery of microRNA-mRNA modules via population-based probabilistic learning. Bioinformatics 23:1141

Kanehisa M, Goto S, Kawashima S, Okuno Y, Hattori M (2004) The KEGG resource for deciphering the genome. Nucleic Acids Res 32:D277–D280

Li Y, Chan EY, Li J, Ni C, Peng X, Rosenzweig E, Tumpey TM, Katze MG (2010) MicroRNA expression and virulence in pandemic influenza virus-infected mice. J Virol 84:3023–3032

Li Y, Li J, Belisle S, Baskin CR, Tumpey TM, Katze MG (2011) Differential microRNA expression and virulence of avian, 1918 reassortant, and reconstructed 1918 influenza A viruses. Virology 421:105–113

Loveday EK, Svinti V, Diederich S, Pasick J, Jean F (2012) Temporaland strain-specific host microRNA molecular signatures associated with swine-origin H1N1 and avian-origin H7N7 influenza A virus infection. J Virol 86:6109–6122

Miller LD, Long PM, Wong L, Mukherjee S, McShane LM, Liu ET (2002) Optimal gene expression analysis by microarrays. Cancer Cell 5:353–361

Neumann G, Kawaoka Y (2001) Reverse genetics of influenza virus. Virology 287:243–250

Ramoni MF, Sebastiani P, Kohane IS (2002) Cluster analysis of gene expression dynamics. PNAS 99:9121–9126

Rogers JV, Price JA, Wendling MQ, Long JP, Bresler HS (2012) Preliminary microRNA analysis in lung tissue to identify potential therapeutic targets against H5N1 infection. Viral Immunol 25:3–11

Schlitt T, Palin K, Rung J, Dietmann S, Lappe M, Ukkonen E, Brazma A (2003) From gene networks to gene function. Genome Res 13:2568–2576

Shalgi R, Lieber D, Oren M, Pilpel Y (2007) Global and local architecture of the mammalian microRNA-transcription factor regulatory network. PLoS Comput Biol 3:e131

Skovgaard K, Cirera S, Vasby D, Podolska A, Breum SØ, Dürrwald R, Schlegel M, Heegaard PM (2013) Expression of innate immune genes, proteins and microRNAs in lung tissue of pigs infected experimentally with influenza virus (H1N2). Innate Immun 19:531–544

Song L, Liu H, Gao S, Jiang W, Huang W (2010) Cellular microRNAs inhibit replication of the H1N1 influenza A virus in infected cells. J Virol 84:8849–8860

Stöhr K (2002) Influenza-WHO cares. Lancet Infect Dis 2:517

Sun S, Zhao G, Xiao W, Hu J, Guo Y, Yu H, Wu X, Tan Y, Zhou Y (2011) Age-related sensitivity and pathological differences in infections by 2009 pandemic influenza A (H1N1) virus. Virol J 8:52

Tambyah PA, Sepramaniam S, Mohamed Ali J, Chai SC, Swaminathan P, Armugam A, Jeyaseelan K (2013) microRNAs in circulation are altered in response to influenza A virus infection in humans. PLoS One 8:e76811

Tan KS, Choi H, Jiang X, Yin L, Seet JE, Patzel V, Engelward BP, Chow VT (2014) Micro-RNAs in regenerating lungs: an integrative systems biology analysis of murine influenza pneumonia. BMC Genom 15:587

Terrier O, Textoris J, Carron C, Marcel V, Bourdon JC, Rosa-Calatrava M (2013) Host microRNA molecular signatures associated with human H1N1 and H3N2 influenza A viruses reveal an unanticipated antiviral activity for miR-146a. J Gen Virol 94:985–995

Wang Y, Brahmakshatriya V, Zhu H, Lupiani B, Reddy SM, Yoon BJ, Gunaratne PH, Kim JH, Chen R, Wang J, Zhou H (2009) Identification of differentially expressed miRNAs in chicken lung and trachea with avian influenza virus infection by a deep sequencing approach. BMC Genom 10:512

Wang Y, Brahmakshatriya V, Lupiani B, Reddy SM, Soibam B, Benham AL, Gunaratne P, Liu HC, Trakooljul N, Ing N, Okimoto R, Zhou H (2012) Integrated analysis of microRNA expression and mRNA transcriptome in lungs of avian influenza virus infected broilers. BMC Genom 13:278

Wright GW, Simon RM (2003) A random variance model for detection of differential gene expression in small microarray experiments. Bioinformatics 19:2448–2455

Wu Z, Hao R, Li P, Zhang X, Liu N, Qiu S, Wang L, Wang Y, Xue W, Liu K, Yang G, Cui J, Zhang C, Song H (2013) MicroRNA expression profile of mouse lung infected with 2009 pandemic H1N1 influenza virus. PLoS One 8:e74190

Xiao S, Mo D, Wang Q, Jia J, Qin L, Yu X, Niu Y, Zhao X, Liu X, Chen Y (2010) Aberrant host immune response induced by highly virulent PRRSV identified by digital gene expression tag profiling. BMC Genom 7:544

Yang H, Crawford N, Lukes L, Finney R, Lancaster M, Hunter KW (2005) Metastasis predictive signature profiles pre-exist in normal tissues. Clin Exp Metastasis 22:593–603

Yi M, Horton JD, Cohen JC, Hobbs HH, Stephens RM (2006) WholePathwayScope: a comprehensive pathway-based analysis tool for high-throughput data. BMC Bioinform 7:30